ATP Sulfurylases from Sulfate-Reducing Bacteria of the Genus Desulfovibrio. A Novel Metalloprotein Containing Cobalt and Zinc †

ARTICLE *in* BIOCHEMISTRY · DECEMBER 1998

Impact Factor: 3.02 · DOI: 10.1021/bi9816709 · Source: PubMed

ATP Sulfurylases from Sulfate-Reducing Bacteria of the Genus *Desulfovibrio.* A Novel Metalloprotein Containing Cobalt and Zinc†

Olga Yu. Gavel,‡,§ Sergey A. Bursakov,‡,§ Juan J. Calvete,|| Graham N. George,⊥ José J. G. Moura,‡ and Isabel Moura*,‡

Departamento de Química, Centro de Química Fina e Biotecnologia, Faculdade de Ciências e Tecnologia, Universidade Nova de Lisboa, 2825 Monte de Caparica, Portugal, Instituto de Investigaciones Biomédicas, CSIC, Valencia, Spain, Stanford Synchrotron Radiation Laboratory, Stanford University SLAC, P.O. Box 4393, Stanford, California 94309, and A. N. Bach Institute of Biochemistry RAS, Lenisky Street 33, 117071 Moscow, Russia

Received July 14, 1998; Revised Manuscript Received September 22, 1998

ABSTRACT: Adenosine triphosphate sulfurylase catalyzes the formation of adenosine 5′-phosphosulfate from adenosine triphosphate and sulfate. The enzyme plays a crucial role in sulfate activation, the key step for sulfate utilization, and has been purified from crude extracts of *Desulfovibrio desulfuricans* ATCC 27774 and *Desulfovibrio gigas*. Both proteins are homotrimers [141 kDa (3 × 47) for *D. desulfuricans* and 147 kDa (3 × 49) for *D. gigas*] and have been identified, for the first time, as metalloproteins containing cobalt and zinc. EXAFS reveals that either cobalt or zinc binds endogenously at presumably equivalent metal binding sites and is tetrahedrally coordinated to one nitrogen and three sulfur atoms. Furthermore, the electronic absorption spectra display charge-transfer bands at 335 and 370 nm consistent with sulfur coordination to cobalt, and as expected for a distorted tetrahedral cobalt geometry, d−d bands are observed at 625, 666, and 715 nm. This geometry is supported by the observation of high-spin Co^{2+} EPR signals at $g \approx 6.5$.

Sulfate is a stable nonreactive compound that must be activated to participate in subsequent metabolic reactions, such as reduction and sulfur transfer. The first activation step in assimilatory and dissimilatory sulfate reduction pathways is accomplished by transferring and coupling the adenosine 5′-phosphoryl moiety of ATP to sulfate (*1*, *2*). This reaction catalyzed by ATP sulfurylase (ATPS)[1] (ATP sulfate adenyltransferase, EC 2.7.7.4) is represented by the equation

$$ATP + SO_4^{2-} \rightleftharpoons APS + PP_i$$

The reduction of sulfate plays a very important role in the sulfur cycle in anaerobic ecosystems such as marine and freshwater environments. The ability to use this quite unreactive molecule (inorganic sulfate) as an external electron acceptor, under moderate environmental conditions, is a common feature of dissimilatory sulfate-reducing bacteria. The dissimilatory process occurring in these organisms involves APS as the active intermediate compound (*3*). In sulfate-reducing bacteria of the genus *Desulfovibrio*, the APS formed is reduced to AMP and sulfite through the mediation of APS reductase (*4*−*6*). Sulfite is then further reduced to hydrogen sulfide, the end product of the sequential reactions. All the enzymes in this pathway are well characterized (*6*, *7*) with the exception of the ATPS(s).

ATPS(s) are widely distributed in nature and have been found in virtually all types of organisms (*8*, *9*), since it was first characterized (*2*, *10*). The enzyme has been partially or extensively purified and characterized from yeast (*11*), *Penicillum chrisogenum* (*12*, *13*), *Penicillum duponti* (*14*), rat liver (*15*), spinach (*16*) and cabbage (*17*) leaves, phototrophic sulfur bacteria (*18*), *Escherichia coli* K12 (*19*), and other sources. ATPS activity has been previously detected in *Desulfovibrio desulfuricans*, *Desulfovibrio gigas*, *Desulfovibrio vulgaris*, *Desulfovibrio africanus*, *Desulfovibrio salexigens*, *Desulfotomaculum orientis*, and *Desulfotomaculum ruminis* (*20*), and ATPS has been partially purified from *D. vulgaris* strain Hildenborough (*21*, *22*) and *Desulfotomaculum nigrificans* (*22*). No reference to the presence of metals in ATPS(s) was made. It appears that this family of enzymes, as isolated from different sources, is quite heterogeneous in terms of amino acid sequence, molecular mass, and subunit composition.

† This work was supported by Praxis XXI Project 2/2.1/QUI/3/94 and Grants BPD/14146/97 and BD/13775/97, and the Stanford Synchrotron Radiation Laboratory is funded by the Department of Energy, Office of Basic Energy Sciences, with further support by the National Institutes of Health, and the Department of Energy, Office of Biological and Environmental Research.

* To whom correspondence should be addressed. Phone: 351-1-2948381. Fax: 351-1-2948550. E-mail: isa@dq.fct.unl.pt.

‡ Universidade Nova de Lisboa.

§ A. N. Bach Institute of Biochemistry RAS.

|| CSIC.

⊥ Stanford University SLAC.

[1] Abbreviations: ATPS(s), adenosine-triphosphate sulfurylase(s); *D.d.*, *D. desulfuricans*; *D.g.*, *D. gigas*; APS, adenosine 5′-phosphosulfate; PEP, phosphoenolpyruvate; EDTA, ethylenediamine-*N*,*N*,*N*′,*N*′-tetraacetic acid; SDS−PAGE, sodium dodecyl sulfate−polyacrylamide gel electrophoresis; Tris, tris(hydroxymethyl)aminomethane; MOPS, 3-(*N*-morpholino)propanesulfonic acid; BSA, bovine serum albumin; PP_i, inorganic pyrophosphate; PPitase, inorganic pyrophosphatase; FPLC, fast protein liquid chromatography; HTP, hydroxyapatite; LMCT, ligand-to-metal charge transfer; EPR, electron paramagnetic resonance; EXAFS, extended X-ray absorption fine structure.

10.1021/bi9816709 CCC: $15.00
Published on Web 10/26/1998

The object of this study is to describe the purification and biochemical and spectroscopic characterization of ATPS(s) isolated from two *Desulfovibrio* species. Both enzymes contain cobalt and zinc, with identical ligation to the metal, and are probably alternatively coordinated at the same binding site. The enzymes can thus be classified as metalloproteins.

MATERIALS AND METHODS

Growth Conditions and Preparation of the Soluble Fraction. D. desulfuricans ATCC 27774 was grown under anaerobic conditions in the medium described by Liu and Peck (*23*) and nitrate used as a terminal electron acceptor. *D. gigas* cells were grown in a basal medium as described by LeGall et al. (*24*), using a lactate/sulfate medium. Cells were harvested at the beginning of the stationary phase (*D. gigas*, 500 g; and *D. desulfuricans*, 900 g), suspended in 10 mM Tris-HCl buffer in a 1/1 ratio (w/v) at pH 7.6, and passed through a Manton-Gaulin press at 9000 psi. The extract was centrifuged at 15000*g* for 1 h; the pellet was then discarded, and the supernatant obtained was termed the crude extract. This extract was subjected to further centrifugation at 180000*g* for 1 h to eliminate the membrane fraction. A clear supernatant, containing the soluble fraction, was then used for the purification of ATPS(s), which were processed immediately.

Purification of ATPS(s). Purification procedures were performed at 4 °C, and the specific activity was determined at each step along the purification process.

D. gigas Enzyme. The soluble fraction was loaded onto an ion exchange DEAE-52 cellulose column (5.5 cm × 36 cm) equilibrated with 10 mM Tris-HCl buffer at pH 7.6. Using a 2 L linear gradient of 10 to 250 mM Tris-HCl at pH 7.6, a fraction containing mainly ATPS activity was eluted at 100−200 mM and concentrated on a Diaflo apparatus with a YM 30 membrane. The ionic strength was decreased by adding 10 mM Tris-HCl buffer (pH 7.6) during the concentration. The next steps of the purification were performed by FPLC (Pharmacia). Ion exchange chromatography was performed using a Source 15Q column (1.6 cm × 22 cm) equilibrated with 10 mM potassium phosphate buffer at pH 7.6. Using a linear gradient of 10 to 500 mM potassium phosphate buffer (pH 7.6) and a flow rate of 4 mL/min over the course of 3 h, a fraction containing mainly ATPS activity was collected at an ionic strength of about 125 mM. The fraction concentrated on a Diaflo apparatus with a YM 30 membrane was loaded onto a Superdex 200 gel filtration column (2.6 cm × 55 cm) equilibrated with 300 mM Tris-HCl buffer (pH 7.6) and eluted with the same buffer with a flow rate of 1 mL/min. The active fraction was pooled and passed through a HTP column (1.6 cm × 20 cm), equilibrated with 300 mM Tris-HCl buffer (pH 7.6). A linear gradient of 1 to 300 mM potassium phosphate buffer (pH 7.6) was applied with a flow rate of 2.5 mL/min over the course of 3 h. Pure ATPS was eluted at about 60 mM.

D. desulfuricans Enzyme. The first purification step was carried out as described above. The active fractions (50−150 mM) were combined and concentrated on a Diaflo apparatus with YM 30 membrane. The ionic strength was decreased by adding 10 mM Tris-HCl buffer (pH 7.6) during the concentration process. The next step was ion exchange FPLC (Pharmacia) performed using a Source 15Q column (2.6 cm × 25 cm) equilibrated with 10 mM Tris-HCl buffer at pH 7.6. A linear Tris-HCl gradient of 10 to 500 mM at pH 7.6 was applied with a flow rate of 3 mL/min over the course of 3 h. Fractions containing mainly ATPS activity were collected at an ionic strength of 50−100 mM. Subsequent steps of purification were as described above, except Superdex 75 was used instead of Superdex 200.

Enzymatic Assay. During purification, the enzymes were assayed by the MgATP synthesis reaction (reverse reaction) via the rate of $NADP^+$ formation (*18*). The reaction was started by addition APS and PP_i after measuring the background rate.

The molybdolysis activity of the enzymes was assayed by measuring the rate of AMP formation at 30 °C via the coupling reaction to NADH oxidation (*15*). The overall stoichiometry is 2 mol of NADH oxidized per mole of AMP formed. The incubation mixture (total volume of 1 mL) conteins 5 mM MgATP, 5 mM excess $MgCl_2$, 20 mM Na_2-MoO_4, 7.5 mM KCl, 0.4 mM PEP, 0.3 mM NADH, 2.5 units/mL PPitase, 30 units/mL myokinase, 40 units/mL pyruvate kinase, and 60 units/mL lactate dehydrogenase. All compounds were prepared in 50 mM Tris-HCl buffer at pH 8.0. The reaction was started by adding MoO_4^{2-} after measuring the background rate.

Typical enzyme concentrations used in analyses with the most higly purified preparations were 0.01−0.03 μg/mL for the molybdolysis and ATP synthesis reactions. One unit of enzyme activity is defined as the amount of enzyme that produces 1 μmol of primary product per minute.

Molecular Mass and Purity Determination. The molecular masses of the purified proteins were determined by gel filtration using a Superdex 200 column (1 cm × 30 cm) with flow rate of 0.5 mL/min. The elution buffer was 50 mM Tris-HCl buffer (pH 7.6) with 150 mM NaCl. The standards used were cytochrome cd_1 from *Pseudomonas nautica* (120 kDa), fuscaredoxin from *D. desulfuricans* ATCC 27774 (58 kDa), and ferritin (440 kDa), catalase (232 kDa), aldolase (158 kDa), BSA (67 kDa), ovalbumin (43 kDa), chymotrypsinogen A (25 kDa), and ribonuclease A (13.7 kDa) (the last seven being purchased from Pharmacia).

Electrospray ionization mass spectrometric analysis was carried out using a Sciex API III Lc-MS/MS system.

The purity and subunit composition were determined by SDS−PAGE at 12.5% (w/v). The proteins used as standards were (from Pharmacia) phosphorylase b (94 kDa), BSA (67 kDa), ovalbumin (43 kDa), carbonic anhydrase (30 kDa), soybean trypsin inhibitor (20.1 kDa), and α-lactalbumin (14.4 kDa). Protein staining was performed using R-250 Coomassie blue.

Spectroscopic Methods. UV−visible absorption data were recorded on a Shimadzu UV-265 split-beam spectrophotometer using 1 cm quartz cells. Low-temperature EPR measurements of the enzymes were taken on an X-band Bruker EMX spectrophotometer equipped with an Oxford Instruments helium liquid flow cryostat.

EXAFS Measurements. X-ray absorption spectroscopic measurements were taken at the Stanford Synchrotron Radiation Laboratory with the SPEAR storage ring containing 55−100 mA at 3.0 GeV. Data were collected on beamline 7-3 using a Si(220) double-crystal monochromator, with an upstream vertical aperture of 1 mm, and a wiggler

field of 1.8 T. Harmonic rejection was accomplished by detuning one monochromator crystal to approximately 50% off peak, and no specular optics were present in the beamline. The incident X-ray intensity was monitored using a nitrogen-filled ionization chamber, and X-ray absorption was measured as the X-ray Kα fluorescence excitation spectrum using an array of 13 germanium intrinsic detectors (*25*). During data collection, samples were maintained at a temperature of approximately 10 K, using an Oxford Instruments liquid helium flow cryostat. For each sample eight to ten 35 min scans were accumulated, and the absorption of a metal foil was measured simultaneously by transmittance. The energy was calibrated with reference to the lowest-energy inflection point of the molybdenum foil, which was assumed to be 7709.5 and 9660.7 eV for Co and Zn, respectively.

EXAFS oscillations $\chi(k)$ were quantitatively analyzed by curve fitting with the EXAFSPAK suite of computer programs [http://ssrl.slac.stanford.edu/exafspak.html] using ab initio theoretical phase and amplitude functions generated with the program *Feff* version 7.02 (*26*, *27*).

Protein Assay. Protein determinations were performed according to the methods of Bradford (*28*) and Lowry et al. (*29*) with BSA as a standard, and also estimated by amino acid composition analysis.

N-Terminal Sequence and Amino Acid Composition Determination. The N-terminal sequences were determined by automated Edman degradation in an Applied Biosystem model 477 A protein sequencer coupled to an Applied Biosystem 120 analyzer following the manufacturer's instructions. A total of 125−200 pmol of ATPS(s) was used. Amino acid analysis was performed with a Pharmacia Alpha Plus amino acid analyzer after hydrolysis for 24 and 48 h in 6 N HCl at 110 °C.

Metal Analysis. Zinc and cobalt levels were determined chemically as indicated in refs *30* and *31*, respectively, and by atomic absorption spectroscopy (Perkin-Elmer 1313, furnace 4100 ZL).

Chemicals and Chromatographic Materials. The biochemicals and enzymes used in the coupled assays were obtained from Sigma: Na-NADP (N-505), NADH (N-8129), APS (A-5508), PEP (P-7002), hexokinase (H-4502), glucose-6-phosphate dehydrogenase (G-4134), myokinase (N-5520), PPitase (I-1643), and a pyruvate kinase/lactate dehydrogenase mixture (P-0294). None of the auxiliary enzymes were desalted before being used. Superdex 75 and Superdex 200 were purchased from Bio-Rad and Source 15Q and HTP from Pharmacia, and DEAE-52 was purchased from Whatman. All other chemicals were of reagent grade at the highest available purity.

RESULTS

Table 1 summarizes the results of purification of the ATPS(s) from *D. desulfuricans* ATCC 27774 and *D. gigas* crude extracts. Both proteins have similar chromatographic behavior, but the *D. gigas* enzyme is more acidic. It was noticed that both proteins are not very stable during purification. The best specific activity obtained for *D. gigas* ATPS, after the Source 15Q column, was 52.9 units/mg at which stage the enzyme was 80% pure according to SDS−PAGE analysis. The final enzyme preparations had specific activities of 28.9 ± 1.1 (*D. gigas*) and 22.5 ± 0.8 units/mg (*D. desulfuricans)*.

Table 1: Purification of ATP Sulfurylases from *D. desulfuricans* ATCC 27774 and *D. gigas*

step	volume (mL)	protein (mg)	activity (units)	specific activity (units/mg of protein)
		D. gigas		
crude extract	1780	64600	155000	2.4
soluble fraction	2180	27900	106000	3.8
DEAE-52	850	7120	98900	13.9
Source 15	420	853	45100	52.9
Superdex 200	29.5	444	10800	24.3
HTP	8	243	7030	28.9
		D. desulfuricans		
crude extract	3200	152000	274000	1.8
soluble fraction	6700	85800	222400	2.6
DEAE-52	810	3720	44200	11.9
Source 15	1366	2780	24200	8.7
Superdex 75	128	696	10800	15.5
HTP	10	222	5000	22.5

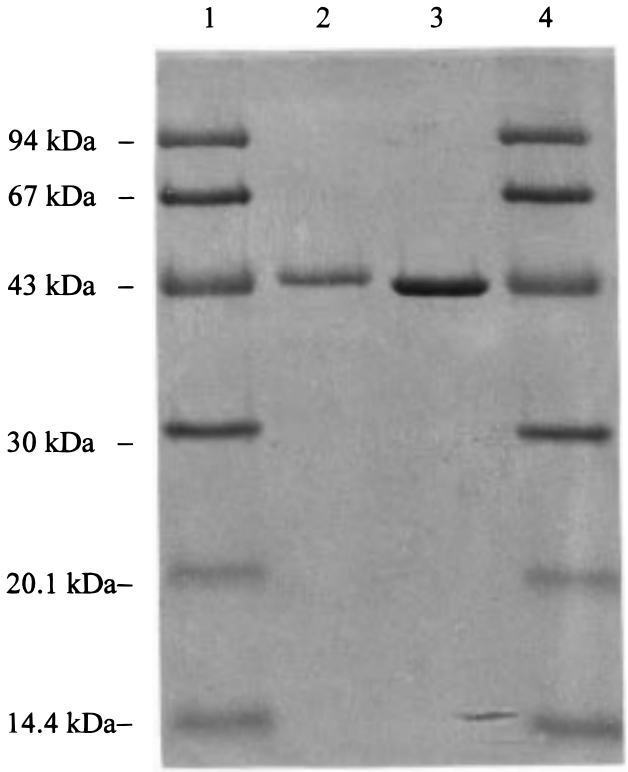

FIGURE 1: SDS−PAGE in 12.5% acrylamide of (lane 2) *D. gigas* (2 μg) and (lane 3) *D. desulfuricans* ATCC 27774 (3 μg) ATPS(s). Lanes 1 and 4 contained the standards.

SDS−PAGE of the pure *D. desulfuricans* and *D. gigas* ATPS(s) disclosed a single dye-stained band with a mobility corresponding to molecular masses of 48 and 50 kDa, respectively (Figure 1). Both enzymes were homogeneous. The molecular masses of the ATPS(s) were also estimated by gel filtration. The protein from *D. desulfuricans* eluted at a K_{av} of 0.316 (138 kDa) and the *D. gigas* enzyme at a K_{av} of 0.307 (151 kDa), suggesting that both enzymes adopt a homotrimer structure under native conditions. The molecular masses of the subunits were also estimated by electrospray mass spectrometry: 47.1 kDa for *D. desulfuricans* and 48−50 kDa for *D. gigas*. The difference between subunit mass determination by different methodologies was not greater than 3%.

One single N-terminal sequence was found for each protein, suggesting that all the subunits are identical. The

Table 2: Amino Acid Composition (moles per 100 mol of total amino acids) of *D. gigas* and *D. desulfuricans* ATCC 27774 ATP Sulfurylases[a]

residue	*D. gigas*	*D. desulfuricans*
Asp and Asn	9.34 (41)	8.49 (36)
Thr	4.28 (19)	3.73 (16)
Ser	3.86 (17)	4.24 (18)
Gln and Glu	11.72 (52)	12.19 (52)
Pro	4.24 (19)	4.68 (20)
Gly	9.59 (42)	9.81 (42)
Ala	10.13 (45)	8.07 (35)
Cys	1.46 (7)	1.05 (5)
Val	7.15 (32)	8.09 (35)
Met	3.64 (16)	4.65 (20)
Ile	4.89 (22)	3.65 (16)
Leu	8.56 (38)	8.76 (38)
Tyr	3.64 (16)	3.08 (13)
Phe	3.65 (16)	3.89 (17)
His	2.17 (10)	2.11 (9)
Lys	7.49 (34)	8.71 (37)
Arg	4.19 (18)	4.81 (21)

[a] The number of residues calculated for *D. gigas* and *D. desulfuricans* enzymes, assuming subunit molecular masses of 49 and 47 kDa, respectively, are shown in brackets.

N termini of both ATPS(s) presented here are not very homologous with the data available in the database: *D. desulfuricans*, KMLSEGAD-VPDHFGRDEVLAILREYYS-GLTEKVEV; and *D. gigas*, AKLVPXHGGKGLVVXLLE-GAELESSV.

Table 2 shows the amino acid composition of *D. desulfuricans* and *D. gigas* enzymes (per monomer) and contains the nearest integer calculated for each residue assuming molecular masses of 47 and 49 kDa, respectively.

Metal analysis of ATPS(s) from both sources indicated the presence of cobalt and zinc. The cobalt and zinc contents (per trimer) were 1.89 ± 0.02 mol of Co and 0.72 ± 0.01 mol of Zn per mole of protein for the *D. desulfuricans* enzyme and 1.53 ± 0.03 mol of Co and 1.38 ± 0.04 mol of Zn per mole of protein for the *D. gigas* enzyme. We can conclude that both enzymes contain close to one metal atom (Co or Zn) per subunit. This is a first indication that cobalt and zinc are probably occupying the same coordination site and some molecules contain cobalt and others contain zinc. This suggestion was further supported by EXAFS measurements (see below).

Incubation of both enzymes in 50 mM MOPS (pH 7.4) with 2×10^{-4} M $CoCl_2$ and 2×10^{-4} M $ZnCl_2$ over the course of 12 and 48 h at 4 °C did not affect the enzymatic activity. Incubation of ATPS(s) with 5 mM EDTA for 24 h in 60 mM phosphate buffer at pH 8.0 at 4 °C did not result in metal chelation and noticeable loss of activity. However, a 10−15% loss of activity was achieved after treatment of 72 h. As a control, ATPS(s) were incubated without EDTA under the same conditions.

ATPS(s) are light blue-greenish in color. The electronic spectra of both purified ATPS(s) are shown in Figure 2. The absorption features and maxima are very similar for both enzymes. They exhibit a protein absorbance band at 279 nm and charge-transfer bands at 335 and 370 nm with d−d band contributions at 625, 666, and 715 nm. The molar extinction coefficients were calculated on the basis of the total cobalt content: $\epsilon_{335} = 4496$ M^{-1} cm^{-1}, $\epsilon_{370} = 2430$ M^{-1} cm^{-1}, $\epsilon_{625} = 598$ M^{-1} cm^{-1}, $\epsilon_{666} = 865$ M^{-1} cm^{-1}, and $\epsilon_{715} = 535$ M^{-1} cm^{-1} for *D. desulfuricans* and $\epsilon_{335} = 4117$ M^{-1} cm^{-1}, $\epsilon_{370} = 2410$ M^{-1} cm^{-1}, $\epsilon_{625} = 460$ M^{-1} cm^{-1}, $\epsilon_{666} = 705$ M^{-1} cm^{-1}, and $\epsilon_{715} = 415$ M^{-1} cm^{-1} for *D. gigas*. Addition of APS, sulfate, and PP_i to pure ATPS(s) preparations in a 1/1 ratio did not induce noticeable changes in the spectra.

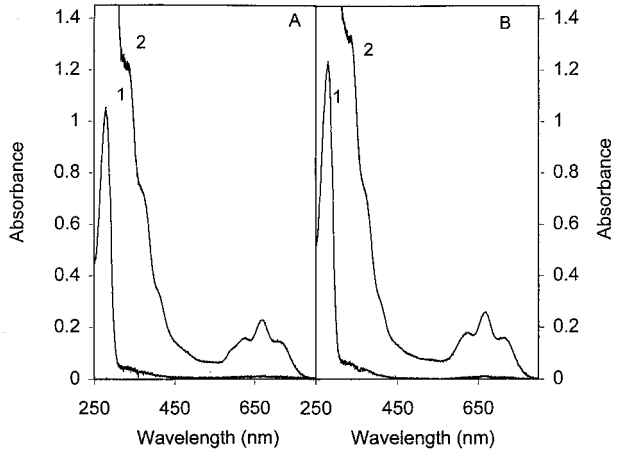

FIGURE 2: Electronic spectra of ATPS(s) from (A) *D. gigas* (1−5.7 μM, 2−200 μM) and (B) *D. desulfuricans* ATCC 27774 (1−7.9 μM, 2−157 μM) in 60 mM potassium phosphate buffer (pH 7.6).

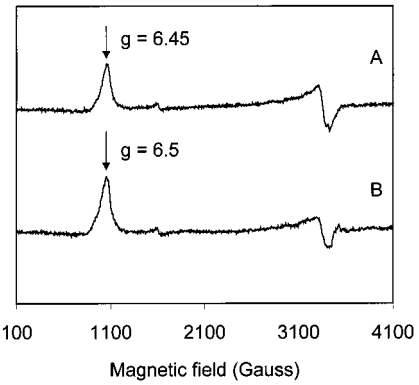

FIGURE 3: EPR spectra of ATPS(s) from (A) *D. gigas* (200 μM, native) and (B) *D. desulfuricans* (200 μM, reduced with 20 mM dithionite) in the 60 mM potassium phosphate buffer (pH 7.6). The spectrum was recorded at 4 K, with a microwave frequency of 9.55 GHz, a microwave power of 2.0 mW, and a modulation amplitude of 10.1.

Figure 3 shows the comparison of the low-temperature X-band EPR spectra of both enzymes. The spectra are very similar, with intense features centered at *g* values of ca. 6.5. The main spectral features were studied in the range of 4−80 K. Their shape was essentially unchanged up to about 30 K and observable, although broadened, up to 50 K. Reduction with dithionite does not affect their intensities. Both ATPS(s) display the same qualitative profile. The spectra are characteristic of high-spin Co(II) ($S = {}^3/_2$) in a rhombically distorted environment with g_{max} values of ≈6.51 for *D. desulfuricans* and 6.45 for *D. gigas* enzymes, respectively. Very minor features assinged to contaminating free high-spin iron(III) (for *D. desulfuricans*) and copper(II) are identified around $g \approx 4.31$ and $g \approx 2.05$ region, respectively. The $g = 4.3$ signal was bleached after dithionite reduction, and the $g = 2$ signal is due to cavity contamination. The EPR spectra arise from the ground Kramers doublet of the $S = {}^3/_2$ multiplet of high-spin Co(II). The observed *g* value

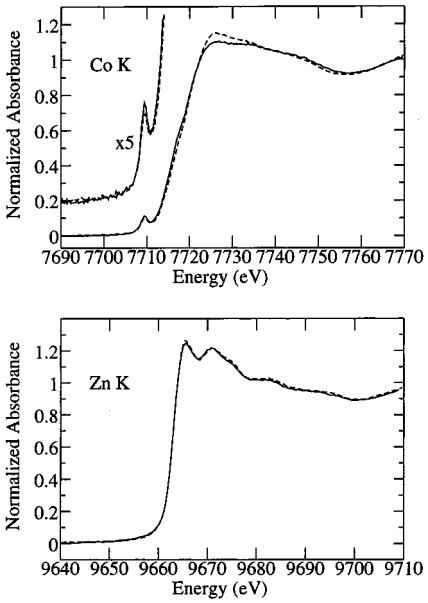

FIGURE 4: Cobalt and zinc X-ray absorption K-edge near-edge spectra of *D. gigas* (broken lines) and *D. desulfuricans* (solid lines) ATPS(s). The inset in the Co K-edge panel shows the 1s → 3d region vertically expanded.

of the EPR spectra is close to that of a pseudotetrahedral complex, but neither the *g* values nor the zero-field splitting parameters are reliable indicators of the geometry. However, spectra are related to those of four-coordinate tetrahedral Co(II) complexes, as observed in model compounds such as $Co(II)(C_2H_5COO^-)_2(imid)_2$ (*32*) and in Co(II)-reconstituted enzymes such as bovine carbonic anhydrase B (*33*), liver alcohol dehydrogenase (*34*), carboxypeptidase A (*35*), the α-fragment of rabbit liver metallothioneine (*36*), Co-desulforedoxin from *D.gigas* (*37*), arthropod hemocyanin (*38*), and azurin from *Pseudomonas aeruginosa* (*39*). Cobalt hyperfine splitting arising from the ^{59}Co nuclear spin ($I = {}^7/_2$) in the low-field region is observed in cobalt-substituted and cobalt-containing proteins (*39*, *40*), but was not detected in our cases.

The EXAFS data of ATPS(s) from *D. desulfuricans* and *D. gigas* complement and clarify the EPR spectral analysis, since the zinc is EPR silent and does not contribute to the electronic spectra. In Figure 4 are compared the X-ray absorption near-edge spectra of the cobalt and zinc K-edges for both *D. gigas* and *D. desulfuricans* ATPS(s). The spectra from the two enzymes are strikingly similar, suggesting almost identical metal coordinations. Both Co K-edge and Zn K-edge spectra are typical of an approximate tetrahedral coordination for the metal. In particular, the Co K-edge spectra show a pronounced 1s → 3d transition at about 7709 eV. This dipole forbidden, quadrupole allowed, transition gains dipole intensity from an admixture of metal 4p states in noncentrosymmetric environments (e.g., tetrahedral symmetry), and its intense presence here supports the notion of an approximately tetrahedral site. For both metals, the spectra show a strong resemblance to those of the approximately tetrahedral sulfur-coordinated model complexes $(NMe_4)_2Co(SPh)_4$ and Zn_2(diethyldithiophosphate)$_4$ (not illustrated), suggesting that the coordination of the metal is predominantly via sulfur ligands.

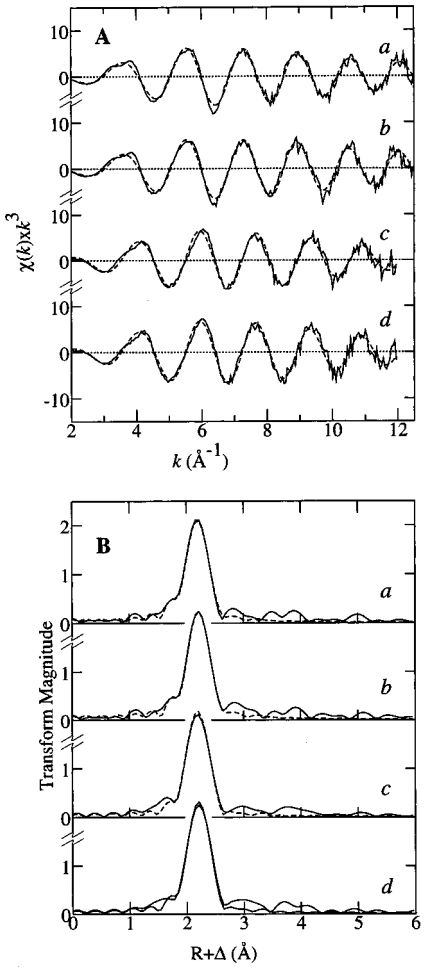

FIGURE 5: (A) EXAFS spectra and (B) EXAFS Fourier transforms (phase-corrected for sulfur backscattering). In all cases, the solid lines show experimental data and the broken lines the best fits. Traces a and b show the Zn K-edge data for *D. gigas* and *D. desulfuricans* ATPS(s), respectively, while traces c and d show Co K-edge data for *D. gigas* and *D. desulfuricans* ATPS(s), respectively.

Figure 5 shows the EXAFS spectra of the Co and Zn sites in *D. gigas* and *D. desulfuricans* ATPS(s), together with the EXAFS Fourier transforms. The data from the two different organisms were again very similar, suggesting a nearly identical metal coordination environment in both. The results of the EXAFS curve-fitting analyses are summarized in Table 3. The curve-fitting analysis gave adequate fits with four sulfur ligands, but in all four cases, the fits were improved slightly by postulating a MS_3N coordination (see Table 3). As the improvement in the EXAFS fit error parameters is, in all four cases, rather subtle, we considered the possibility that this was an artifact of analysis, perhaps due to the inadequacy of the ab initio theoretical phase and amplitude functions that were employed. We therefore attempted to fit the Zn EXAFS of zinc-substituted rubredoxin (*42*), which is known to be a ZnS_4 site, with a ZnS_3N model, using a *k* range identical to the ATPS data. When this was done, the EXAFS error parameter increased from 0.235 for ZnS_4 to 0.243 for ZnS_3N. Further support for the postulated N donor ligand can be obtained from examination of the long *R* features in the EXAFS Fourier transform. In Figure 6, the Zn K-edge EXAFS Fourier transform of *D. desulfuricans* ATPS is compared with that of a [Zn(imidazole)$_4$] model

Table 3: EXAFS Curve-Fitting Analysis[a]

	M−S distance			M−N distance				
sample	*N*	*R* (Å)	σ^2 (Å^2)	*N*	*R* (Å)	σ^2 (Å^2)	ΔE_0(eV)	error[b]
D.g. Zn	4	2.301 (2)	0.0054 (1)				−16.8 (6)	0.243
	3	2.309 (3)	0.0034 (2)	1	2.061 (13)	0.0024[c]	−16.6 (8)	0.232
D.d. Zn	4	2.311 (3)	0.0049 (1)				−15.4 (6)	0.261
	3	2.318 (3)	0.0030 (2)	1	2.070 (14)	0.0024[c]	−15.0 (8)	0.246
D.g. Co	4	2.269 (3)	0.0062 (2)				−11.8 (6)	0.274
	3	2.287 (3)	0.0048 (3)	1	2.071 (13)	0.0025[c]	−9.3 (6)	0.266
D.d. Co	4	2.278 (3)	0.0058 (2)				−10.1 (6)	0.292
	3	2.291 (3)	0.0039 (2)	1	2.051 (15)	0.0025[c]	−9.0 (8)	0.276

[a] The values in parentheses are the estimated standard deviations (precisions) obtained from the diagonal elements of the covariance matrix. We note that the accuracies will always be somewhat larger than the precisions, typically ±0.02 Å for *R* and ±20% for *N* and σ^2. Note that EXAFS cannot readily distinguish between scatterers with similar atomic numbers, such as chlorine and sulfur, or nitrogen and oxygen. [b] The fit error is defined by equation $\Sigma k^6(\chi_{exptl} - \chi_{calcd})^2/\Sigma k^6\chi_{exptl}^2$. [c] The Zn−N σ^2 value showed high mutual correlation in the refinements with that of the Zn−S EXAFS and could not be independently refined. The Zn−N σ^2 value was therefore fixed at the value estimated for Zn−imidazole coordination (A. V. Poiarkova and J. J. Rehr, personal communication; *41*).

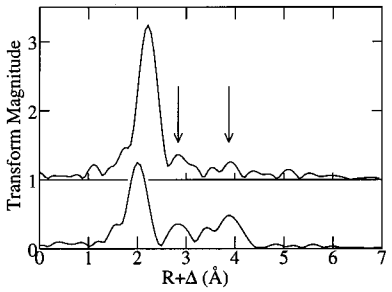

FIGURE 6: Comparison of Zn K-edge EXAFS Fourier transforms of *D. desulfuricans* ATPS and that of Zn[imidazole]$_4$, Zn−S phase corrected for comparison with Figure 7. The arrows indicate Fourier transform features that can be attributed in the model to outer shell C and N from the imidazole ring. Similar features can be seen with the enzyme data.

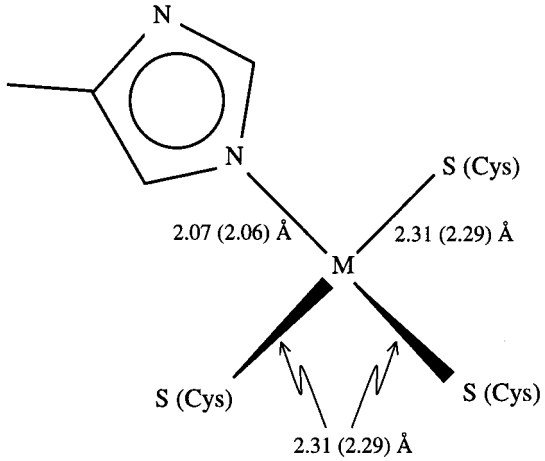

FIGURE 7: Postulated structure for Co and Zn sites of *D. gigas* and *D. desulfuricans* (solid lines) ATPS(s). In the figure, M is either Co or Zn and bond lengths are the average of the *D. gigas* and *D. desulfuricans* Zn values, with values in parentheses the average for Co.

complex. Although the signal-to-noise ratio of the enzyme data did not allow us to attempt a quantitative analysis, some similarity of the outer shell Fourier transform peaks (indicated) is clearly visible. These features are due to single and multiple scattering involving the outer carbons and nitrogens of the imidazole ring and are characteristic of histidine coordination in metalloproteins. While the intensity of these features in the enzyme spectra is close to that of the noise, they remain when the *k* range of the Fourier trasform is reduced, and when Gaussian *k* space window functions were applied, indicating that they are not artifacts due to noise or series termination effects.

A search of the Cambridge Crystallographic Data Base indicated that the bond lengths determined (in Table 3) were typical of four-coordinate metal thiolate sites for which typical M−S bond lengths were 2.36 and 2.31 Å for Zn and Co, respectively. For zinc, but not for cobalt, a model exists with three thiolates and one imidazole ligand (*43*). This compound has Zn−S and Zn−N bond lengths of 2.36 and 2.06 Å, respectively, which are in good agreement with the values determined from EXAFS curve fitting (Table 3). A postulated structure for the metal site is shown in Figure 7.

DISCUSSION

The isolation and the characterization of the enzyme responsible for the activation of the sulfate molecule are key steps in the understanding of one of the most primitive respiratory chains. Furthermore, the enzyme was identified as a metalloprotein. The enzymatic activities associated with the pure ATPS(s) from *D. desulfuricans* and *D. gigas* are on the order of the specific activities found in other systems [in the direction of ATP production values of ATPS(s) activities from different sources are 20 units/mg (rat liver) (*15*), 38 units/mg (cabbage leaf) (*17*), 48 units/mg (*D. vulgaris* Hildenborough) (*21*), and 50 units/mg (*P. duponti*) (*14*) and in the specific molybdolysis activities are 68 units/mg (*D. vulgaris* Hildenborough) (*22*), 24 units/mg (*P. chrisogenum*) (*12*), 20 units/mg (*P. duponti*) (*14*), 20 units/mg (rat liver) (*15*), and 8.3 units/mg (*Dm. nigrificans*) (*22*)].

The molecular masses of native ATPS(s) vary with the species and have a monomeric (*44*), dimeric (*17*), tetrameric (*16*), and hexameric (*12*, *14*) organization. Most of the ATPS(s) have identical subunit compositions, in contrast to *E. coli* K12 enzyme which is composed of two different subunits (*17*). ATPS(s) from *D. desulfuricans* and *D. gigas* are homotrimers with approximate molecular masses of 141 (3 × 47) and 147 (3 × 49) kDa. These subunit sizes are similar to those of the spinach leaf (49−50 kDa) (*16*) and trophosome tissue of hydrothermal vent tube worm (48 kDa) (*45*) enzymes but smaller than those of the subunits from fungi, rat liver, and yeast (62−69 kDa) (*11*, *12*, *14*, *15*). ATPS(s) from different sulfate reducers seem to have quite distinct behaviors in terms of electrophoretic mobility (*20*).

Dissimilatory ATPS(s) from *D. desulfuricans* and *D. gigas* contain 5 and 7 cysteines and 20 and 16 methionines, respectively. Sulfate assimilators contain relatively few sulfur amino acid residues (1−3 cysteines and 6−12 methionines) (*46*) in contrast with the *Riftia* symbiont enzyme which contains 7 cysteines and 21 methionines (*47*). This suggests that dissimilatory ATPS(s) are more closely related to the chemolitotrophs in terms of sulfur-containing amino acids.

The visible absorbance spectra of ATPS(s) either originate from electronic transitions between electronic energy levels of the metal binding sites (d−d transition due to Co^{2+}) or are electronic transitions from electronic levels of the ligand to the energy levels of the metal. The low-wavelength absorbance is assigned to a LMCT band indicative of sulfur-to-cobalt charge transfer resulting from thiolate coordination (*48*). The charge-transfer bands from the ligand to zinc will be located around 225 and 275 nm and will be hidden by the protein absorbance bands that have a higher extinction coefficient (*49*). The near-ultraviolet LMCT band lies at 335 nm with a molar absorptivity of 4496 M^{-1} cm^{-1} for *D. desulfuricans* and 4117 M^{-1} cm^{-1} for *D. gigas*, and is assigned to charge-transfer transitions from the bound ligands' sulfur to Co^{2+}. The extinction coefficients of LMCT bands are normally 900−1300 M^{-1} cm^{-1} per cobalt−thiolate bond (*50*). Therefore, we can conclude that cobalt is bound to at least three sulfur groups. The positions and intensities of bands at 335, 666, and 715 nm are comparable to those of known tetrahedral Co^{2+} complexes with three or four thiolate ligands, e.g., inorganic tetrathiolate−Co^{2+} complexes (*49*, *51*) and Co^{2+}-substituted metalloproteins such as horse liver alcohol dehydrogenase with Co^{2+} bound at the non-catalytic metal binding site (*52*), rabbit liver $Co(II)_7$−metallothionein (*53*), Co^{2+}−rubredoxin (*37*, *50*), Co^{2+}−desulforedoxin (*37*), and the α-fragment of rabbit liver Co^{2+}−metallothionein (*36*). We suggest that both *Desulfovibrio* ATPS(s) have most probably three sulfur atoms coordinating the cobalt. EXAFS data confirm that zinc is in a similar environment (see below). Also, the spectra of ATPS(s) from *D. desulfuricans* and *D. gigas* are somewhat similar with the spectrum of bromoperoxidase from *Pseudomonas putida* that contains cobalt (*54*).

The following questions are to be raised at this point: are zinc and cobalt part of a binuclear site, are zinc and cobalt occupying different and/or independent sites, or are zinc and cobalt alternating at the same coordination site? The analysis of the EXAFS data of ATPS(s) from both sources shows that both cobalt and zinc are four-coordinated by three sulfurs and one nitrogen. No short metal−metal distances are detected, confirming the mononuclear nature of the sites. Due to the insufficient number of cysteines per molecule, this would mean that the molecules contain either zinc or cobalt at the same coordination site. The *D. desulfuricans* enzyme has less zinc than cobalt (1/2.6), and the *D. gigas* enzyme has equal amounts of zinc and cobalt (1/1).

The metal determinations and the analysis of the UV−visible spectrum, EPR, and EXAFS data indicate that each monomer has only one metal binding site (for cobalt or zinc) that provides a sulfur−nitrogen coordination sphere to the metal (most probably cysteinyl and histidinyl ligation). Both metals are required, probably, for activity since the activities of the enzymes decrease after treatment with EDTA for long periods of time. The activity of the pure ATPS(s) could not be increased by adding Co^{2+}, Zn^{2+}, or both.

Cobalt and zinc are necessary as trace elements in all cells but can be toxic at higher concentrations. Cobalt is a central metal cofactor in the corrin ring of vitamin B_{12} and plays important roles in a wide range of biological functions. This ion is present in many noncorrinoid enzymes such as methionyl aminopeptidase (*55*), transcarboxylase (*56*), lysine 2,3-aminomutase (*40*), nitrile hydratase (*57*), bromoperoxidase (*54*), amidase (*58*), and cobalt transport proteins (*59*). Zinc is present in more than 300 enzymes, which contain a single Zn^{2+} ion, several Zn^{2+} ions, or different metal ions, including Zn^{2+}. Zinc and cobalt can be intersubstituted and display activities comparable to that of the native enzyme (*60*). Both metals in ATPS(s) from *D. desulfuricans* and *D. gigas* can be functional and necessary for the catalytic action and/or structure and even not involved in the catalytic mechanism but necessary to keep the protein in the proper conformation.

The enzymes characterized from two sulfate reducers from the genus *Desulfovibrio* are quite similar in terms of masses, specific activities, and metal coordination spheres. The presence of the two different metals, cobalt and zinc in ATPS(s), means these proteins are related to the diverse family of the Zn-containing enzymes and also to the small group of Co-containing enzymes (excluding the distinct family of cobalamin proteins). This is the first report describing ATPS(s) as metalloproteins. The EPR and electronic spectra are compatible with the EXAFS results and are indicative of high-spin Co^{2+} in a tetrahedral coordination. Zinc is diamagnetic and is not observed by EPR. From the metal analysis and the results obtained from EXAFS, we can conclude that cobalt and zinc are probably occupying the same coordination sites. The total metal content is very close to three per trimer, suggesting that each monomer has a full metal complement. This is also consistent with the fact that, after incubation with extra metal, no alterations are observed in the specific activity or in the visible spectra.

ACKNOWLEDGMENT

We are grateful to R. Toci for growing the cells used in this work and S. Besson for providing the cytochrome cd_1. We thank our colleagues G. Fauque, C. Brondino, and R. Franco for helpful discussions. We are indebted to Martin J. George of SSRL for use of his data collection software and to Ingrid J. Pickering of SSRL for assistance with data collection.

REFERENCES

1. Wilson, L. G., and Bandursky, R. S. (1958) *J. Biol. Chem. 233*, 975−981.
2. Robbins, P. W., and Lipmann, F. (1958) *J. Biol. Chem. 233*, 686−690.
3. Peck, H. D., Jr. (1962) *Bacteriol. Rev. 26*, 67−94.
4. Ishimoto, M., and Fujimoto, D. (1961) *J. Biochem. (Tokyo) 50*, 299−304.
5. Still, W., and Trüper, H. G. (1984) *Arch. Microbiol. 137*, 145−150.
6. Lampreia, J., Pereira, A. S., and Moura, J. J. G. (1994) *Methods Enzymol. 243*, 241−260.
7. Hynh, B. H. (1994) *Methods Enzymol. 243*, 523−543.

8. Mulder, G. J. (1982) in *Sulfation of drugs and related compounds* (Mulder, G. J., Ed.) pp 56−69, CRC Press, Boca Raton, FL.
9. Leyh, T. S. (1993) *Crit. Rev. Biochem. Mol. Biol. 28*, 515−542.
10. Robbins, P. W., and Lipmann, F. (1958) *J. Biol. Chem. 233*, 681−685.
11. Hawes, C. S., and Nicolas, D. J. D. (1973) *Biochem. J. 133*, 541−550.
12. Renosto, F., Martin, R. L., Wailes, L. M., Daley, L. A., and Segel, I. H. (1990) *J. Biol. Chem. 265*, 10300−10308.
13. Seubert, P. A., Grant, P. A., Christie, E. A., Farley, J. R., and Segel, I. H. (1979) *Ciba Found. Symp. 72*, 19−47.
14. Renosto, F., Schultz, T., Re, E., Mazer, J., Chandler, C. J., Barron, A., and Segel, I. H. (1985) *J. Bacteriol. 164*, 674−683.
15. Yu, M., Martin, R. L., Jain, S., Chen, L. J., and Segel, I. H. (1989) *Arch. Biochem. Biophys. 269*, 156−174.
16. Renosto, F., Patel, H. C., Martin, R. L., Thomassian, C., Zimmerman, G., and Segel, I. H. (1993) *Arch. Biochem. Biophys. 307*, 272−285.
17. Osslund, T., Chandler, C., and Segel, I. H. (1982) *Plant Physiol. 70*, 39−45.
18. Dahl, C., and Trüper, H. G. (1994) *Methods Enzymol. 243*, 400−421.
19. Leyh, T. S., Taylor, J. T., and Markham, G. H. (1987) *J. Biol. Chem. 263*, 2409−2416.
20. Skyring, G. W., Trudinger, P. A., and Shaw, W. H. (1972) *Anal. Biochem. 48*, 259−265.
21. Baliga, B. S., Vartak, H. G., and Jagannathan, V. (1961*) J. Sci. Ind. Res.* (*India*) *20C*, 33−40.
22. Akagi, J. M., and Campbell, L. L. (1962) *J. Bacteriol. 84*, 1194−1201.
23. Liu, M. C., and Peck, H. D., Jr. (1981) *J. Biol. Chem. 256*, 13159−13164.
24. LeGall, J., Mazza, G., and Dragoni, N. (1965) *Biochim. Biophys. Acta 99*, 385−387.
25. Cramer, S. P., Tench, O., Yocum, M., and George, G. N. (1988) *Nucl. Instrum. Methods Phys. Res. A266*, 586−591.
26. Rehr, J. J., Mustre de Leon, J., Zabinsky, S. I., and Albers, R. C. (1991) *J. Am. Chem. Soc. 113*, 5135−5140.
27. Mustre de Leon, J., Rehr, J. J., Zabinsky, S. I., and Albers, R. C. (1991) *Phys. Rev. B44*, 4146−4156.
28. Bradford, M. M. (1976) *Anal. Boichem. 72*, 248−254.
29. Lowry, O. H., Rosenbrough, N. J., Farr, A. L., and Randall, R. J. (1951) *J. Biol. Chem. 193*, 265−275.
30. Homsher, P., and Zak, B. (1985) *Clin. Chem. 31*, 1310−1313.
31. Evans, C. H. (1983) *Anal. Biochem. 135*, 335−339.
32. Horrocks, W. D., Jr., Ishley, J. N., Holmquist, B., and Thomson, J. S. (1980) *J. Inorg. Biochem. 12*, 131−141.
33. Grell, E., and Bray, R. S. (1971) *Biochim. Biophys. Acta 236*, 503−506.
34. Makinen, M. W., and Yim, M. B. (1981) *Proc. Natl. Acad. Sci. U.S.A. 78*, 6221−6225.
35. Martinelli, R. A., Hanson, G. R., Thompson, J. S., Holmquist, B., Pilbrow, J. R., Auld, D. S., and Vallee, B. L. (1989) *Biochemistry 28*, 2251−2258.
36. Good, M., and Vašák, M. (1986) *Biochemistry 25*, 3328−3334.
37. Moura, I., Teixeira, M., LeGall, J., and Moura, J. J. G. (1991) *J. Inorg. Biochem. 44*, 127−139.
38. Bubacco, L., Magliozzo, R. S., Beltramini, M., Salvato, B., and Peisach, J. (1992) *Biochemistry 31*, 9294−9303.
39. Bonander, N., Vänngård, T., Tsai, L.-C., Langer, V., Nar, H., and Sjölin, L. (1997) *Proteins: Struct., Funct., Genet. 27*, 385−394.
40. Petrovich, R. M., Ruzicka, F. J., Reed, G. H., and Frey, P. A. (1991) *J. Biol. Chem. 266*, 7656−7660.
41. Loeffen, P. W., Pettifer, R. F., and Tomkinson, J. (1996) *Chem. Phys. 208*, 403−409.
42. George, G. N., Pickering, I. J., Prince, R. C., Zhou, Z.-H., and Adams, M. W. W. (1996) *J. Biol. Inorg. Chem. 1*, 226−230.
43. Gruff, E. S., and Koch, S. A. (1989) *J. Am. Chem. Soc. 111*, 8762.
44. Li, J., Saidha, T., and Schiff, J. A. (1991) *Biochim. Biophys. Acta 1078*, 68−76.
45. Renosto, F., Martin, R. L., Borrell, J. L., Nelson, D. C., and Segel, I. H. (1991) *Arch. Biochim. Biophys. 290*, 66−78.
46. Foster, B. A., Thomas, S. M., Mahr, J. A., Renosto, F., Patel, H. C., and Segel, I. H. (1994) *J. Biol. Chem. 269*, 19777−19786.
47. Laue, B. E., and Nelson, D. C. (1994) *J. Bacteriol. 176*, 3723−3729.
48. Bertini, I., and Luchinat, C. (1984) *Adv. Inorg. Biochem. 6*, 71−111.
49. Swenson, D., Baenziger, L. N., and Coucouvanis, D. (1978) *J. Am. Chem. Soc. 100*, 1932−1934.
50. May, W., and Kuo, J. Y. (1978) *Biochemistry 17*, 3333−3338.
51. Lane, R. W., Ibers, J. A., Frankel, R. B., Papaefthymiou, G. C., and Holm, R. H. (1977) *J. Am. Chem. Soc. 99*, 84−98.
52. Maret, W., Andersson, I., Dietrich, H., Schneider-Bernlöhr, H., Einarsson, R., and Zeppezauer, M. (1979) *Eur. J. Biochem. 98*, 501−512.
53. Vašák, M., Kagi, G. N. R., Holmquist, B., and Vallee, B. L. (1981) *Biochemistry 20*, 6659−6664.
54. Itoh, N., Morinaga, N., and Kouzai, T. (1994) *Biochim. Biophys. Acta 1207*, 208−216.
55. Arfin, S. M., Kendall, R. L., Hall, L., Weaver, L. H., Stewart, A. E., Matthews, B. W., and Bradshaw, R. A. (1995) *Proc. Natl. Acad. Sci. U.S.A. 92*, 7714−7718.
56. Harmon, F. R., Goss, N. H., and Wood, H. G. (1982) *Biochemistry 21*, 2847−2852.
57. Nagasawa, T., Takeuchi, K., and Yamada, H. (1988) *Biochem. Biophys. Res. Commun. 155*, 1008−1016.
58. Nawaz, M. S., Khan, A. A., Bhattacharayya, D., Siitonen, P. H., and Cerniglia, C. E. (1996) *J. Bacteriol. 178*, 2397−2401.
59. Komeda, H., Kobayashi, M., and Shimizu, S. (1997) *Proc. Natl. Acad. Sci. U.S.A. 94*, 36−41.
60. Bertini, I. (1983) in *The Coordination Chemistry of Metalloenzymes* (Bertini, I., Drago, R. S., and Luchinat, C., Eds.) pp 1−18, D. Reidel Publishing Co., Dordrecht, The Netherlands.

BI9816709